https://doi.org/10.6113/TKPE.2019.24.5.311

Tx-Rx간 무선통신이 필요 없는 LLC 컨버터 기반 유도형 무선전력전송 시스템 구현

김문영†, 최신욱[1], 강정일[1], 한종희[1]

Implementation of Inductive Wireless Power Transfer System based on LLC Converter without Wireless Communication between Tx and Rx

Moon-Young Kim†, Shin-Wook Choi[1], Jeong-il Kang[1], and Jonghee Han[1]

Abstract

In general wireless power transfer systems (WPTSs), power transfer is controlled by the wireless communication between a transmitter (Tx) and a receiver (Rx). However, WPTS is difficult to apply in electronic products that do not have batteries, such as TVs. A WPTS with resonators based on a transformer of LLC series resonant converter is proposed in this study to eliminate wireless communication units between a Tx and an Rx. The proposed system operates at the boundary of the resonance frequency, and the required power can be stably supplied to authorized devices even though some misalignment occurs. Moreover, standby power standards for the electronic product can be satisfied.

Key words: IPT(Inductive Power Transfer), LLC series resonant converter, Wireless power transfer, WPTS (Wireless Power Transfer System)

1. Introduction

A wireless power transfer (WPT) is power transmission technology without an electrical conductor between source and load. A typical wireless power transfer system (WPTS) consists of a transmitter (Tx) and a receiver (Rx) as shown in Fig. 1[1]-[3]. The transmitter transmits power received from an AC inlet to the receiver, and the receiver provides the power from the transmitter to the load [1]-[3].

The transmitter is composed of a PFC converter, an inverter and their controllers. The inverter circuit converts the DC output voltage of the PFC circuit into a high-frequency AC power signal. The inverter controller controls the inverter based on information

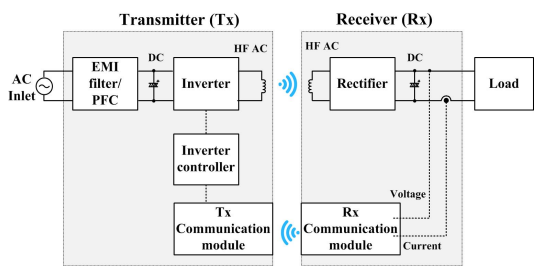

Fig. 1. A typical wireless power transfer system.

received from the receiver through wireless communication. The receiver has a rectifier circuit to convert high-frequency AC power into a DC power. A communication module is also needed to transmit receiver's voltage and current information to the transmitter[4]-[6].

Generally, feedback control is required to supply the proper power to the load. However, in WPTS, Tx and Rx are physically separated. Therefore, a wireless communication modules for feedback control are essential in the Tx and Rx respectively. However, it increases system implementation cost and size, and a definite wireless communication protocol is required

Paper number: TKPE-2019-24-5-1
Print ISSN: 1229-2214 Online ISSN: 2288-6281
† Corresponding author: moon.y.kim@samsung.com, Visual Display Business, Samsung Electronics Co., Ltd.
Tel: +82-31-277-0207
[1] Visual Display Business, Samsung Electronics Co., Ltd.
Manuscript received Feb. 21, 2019; revised Mar. 11, 2019; accepted Apr. 6, 2019
— 본 논문은 2018년 추계학술대회 우수추천논문임

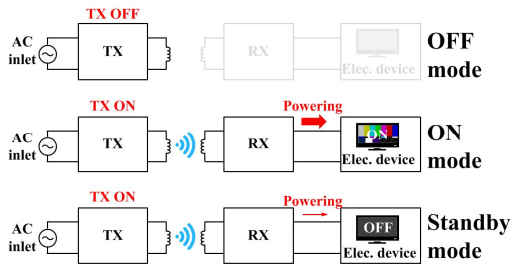

Fig. 2. WPT for electronic device requiring standby mode.

between Tx and Rx. In addition, the battery in the Rx is also required for standby to recognize Tx signals, so it is obliged to add a battery into a product such as a TV that does not usually use the battery.

In contrast with the wireless charging system, most electronic devices require a standby mode as shown in Fig. 2, and thus the standby power should also be supplied by WPT. However, WPTS normally has low efficiency at light load conditions [7]-[12]. Moreover, the wireless communication module itself increases the standby power consumption. As a result, it is difficult to satisfy standby requirements in the standby mode on WPT system.

Therefore, in this paper, we propose an inductive wireless power transmission system based on LLC converter to eliminate the wireless communication module between Tx and Rx.

2. Proposed Wireless Power Transfer System

2.1 System structure

The proposed wireless power transfer system is shown in Fig. 3. The resonator is designed based on the LLC converter. The inverter circuit performs the open loop operation in a designed frequency range near the resonance frequency of resonator. In other words, the inverter operates at a spreading frequency near the resonance frequency for EMI reduction, rather than a fixed frequency. To compensate for the elimination of wireless communication, a minimum of protection circuitry, such as under voltage protection, is required. ON/OFF signal between Tx and Rx is also required for protection and the standby mode. And, an Rx detection circuit is also required.

2.2 Operational principle

Due to the outer case surrounding the Tx and Rx devices, the resonators have above a certain distance from each other. Thus low coupling caused by separation distance provides sufficient leakage inductance

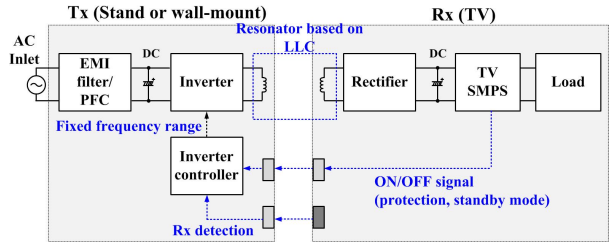

Fig. 3. Structure of proposed WPT system.

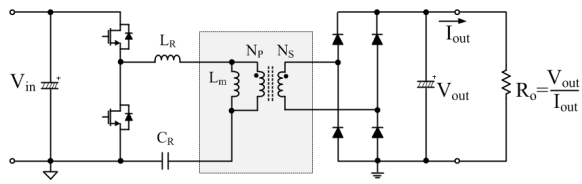

Fig. 4. Circuit diagram of LLC converter.

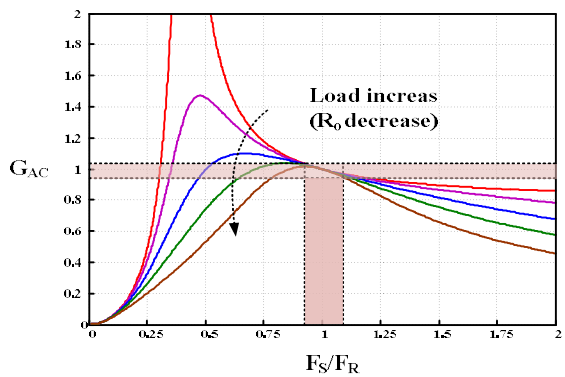

Fig. 5. Voltage gain according to output load.

(L_R) for resonance. If the resonators can be designed with wide area enough to have a inductance similar to magnetic inductance (L_m) of a transformer, the resonator of the proposed WPTS can have an equivalent circuit similar to the transformer of the LLC converter. Therefore the proposed system can have the same output voltage gain characteristics with the LLC converter. Fig. 4 shows the LLC converter with full-bridge rectifier. The voltage gain of LLC converter can be obtained from Fundamental Harmonic Approximation (FHA) as follow:

$$G_{DC}=\frac{Vout}{Vin}=\frac{G_{AC}}{2n}=\frac{1}{2n\sqrt{\left\{1+\frac{1}{m}\left[1-\left(\frac{F_R}{F_S}\right)^2\right]\right\}^2+\left[\left(\frac{F_S}{F_R}-\frac{F_R}{F_S}\right)\frac{\pi^2}{8n^2}Q\right]^2}} \quad (1)$$

$$n=\frac{N_P}{N_S},\ F_R=\frac{1}{2\pi\sqrt{L_RC_R}},Q=\sqrt{\frac{L_R}{C_R}}\frac{1}{R_o},\ m=\frac{L_m}{L_R}$$

From equation (1), voltage gain according to output load can be plotted as shown in Fig. 5[13],[14]. When the LLC converter operates near the resonant frequency, the output voltage gain is nearly constant regardless

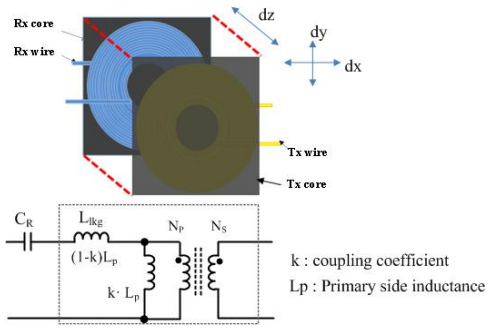

Fig. 6. Misalignment of resonators.

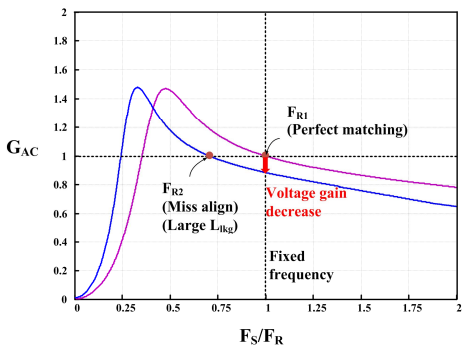

Fig. 7. Voltage gain variation according to position between Tx and Rx.

of output load condition. Therefore, the inverter of the proposed system can be operated with open loop.

Fig. 6 shows misalignment of two resonators and their equivalent circuit. The coupling between Tx and Rx resonators is reduced when the distance of the two resonators is farther in the z-axis direction and not perfectly aligned in the x-y axis. The value of the leakage inductance (L_R) participating in the resonance increases due to the reduced coupling. Since the resonance capacitor (C_R) has a fixed value irrespective of the resonator position, the resonance frequency of the resonator becomes lower due to the increased leakage inductance. In the proposed system, the inverter operates in the fixed frequency range. As a result, the output voltage of WPTS becomes lower as shown in Fig. 7.

When two resonators are perfectly aligned in the x-y axis and have the minimum distance in z-axis, the voltage gain is the highest theoretically, so an over-voltage protection circuit is not required in the well-designed system.

As described above, the farther the distance between two resonators is, the lower the transmitted voltage is. However, even if the voltage gain is lowered, the power transmission is possible. In particular,

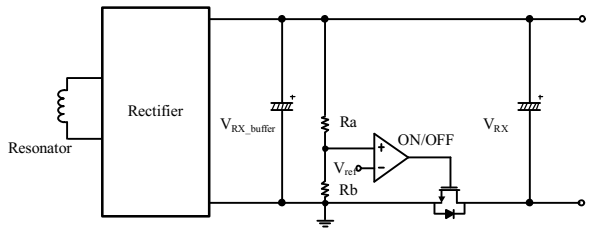

Fig. 8. Under voltage protection circuit.

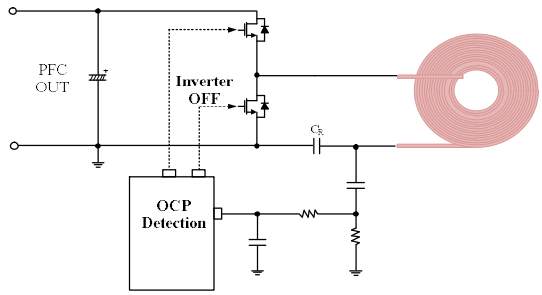

Fig. 9. Over current protection circuit.

products such as TVs with downstream converters (i.e. LED drivers) are able to operate without complete control for the output voltage regulation of the wireless power transfer.

3. System Implementation Considerations

3.1 Under-voltage protection (UVP) circuit

If the transmitted voltage is decreased due to the misalignment of resonators, the current will increase for delivering the same power. As a result, it will cause increase of the current stress of the Rx devices. In order to prevent current increase more than necessary, under-voltage protection circuit (UVP) is required and it should be automatically operated without wireless communication.

Fig. 8 shows an example of an UVP circuit implemented with a semiconductor switching device. In the illustrated circuit, when the received voltage (V_{RX_buffer}) reaches to a certain level, the FET operates and the voltage is transmitted to the next stage (V_{RX}). In other words, the receiver automatically blocks power receiving from the transmitter if it does not satisfy a sufficient alignment state. At this time, considering the standby power, R_a and R_b should be designed to have a sufficiently large value.

3.2 Over-current protection (OCP) circuit

Fig. 9 shows example of over-current protection circuit. Over-current can be measured on the Tx side as same manner of LLC converter.

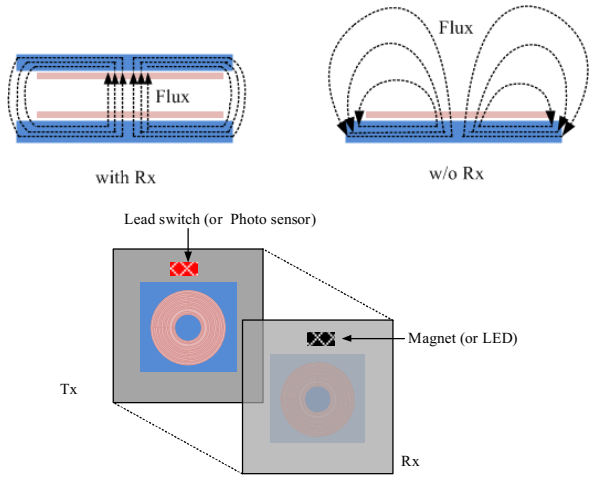

Fig. 10. Necessity of Rx detection and its apparatus.

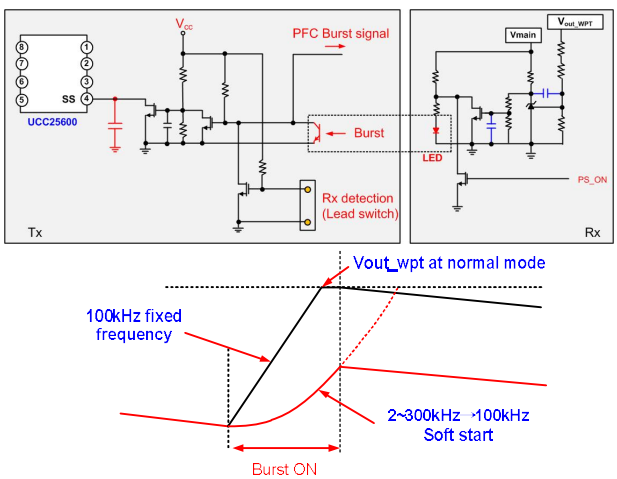

Fig. 11. Burst operation using soft-start pin for standby power consumption.

3.3 Rx detection

If the receiver is not installed, the transceiver will cause unnecessary power loss if the Tx coil continues to operate as shown in Fig. 10. In addition, serious problems can occur, especially when other commercial devices containing magnetic components for wireless charging are nearby. Therefore, the Tx should selectively transmit power only to the matched receiver using Rx detection circuit.

The Rx detection circuit can be implemented by using the magnet and the magnetic switch in the matched coordinates as shown in Fig. 10. Or, an LED emitting a specific wavelength and a photo sensor can be also used. In the case of a magnet, since the user may accidentally place other magnets at an arbitrary point, several sensing units should be provided to prevent this. And the Tx should operate only when all sensing points are detected.

3.4 Standby circuit with low burst frequency

In the case of TV, since the remote control receiver is generally on the Rx side, a signal transfer from Rx to Tx is necessary to enter the standby mode. Therefore, an additional device is needed to recognize the standby mode because there is no circuit for wireless communication in the proposed system. As shown in Fig. 11, a device for the standby signal can be realized by an LED and an LED light receiving unit. Burst operation using a soft-start function of the control IC to reduce standby power consumption is required as shown in Fig 11. When PS_ON signal is low level and so the LED is turned on, the operation of inverter stops. Generally, since the light load efficiency of WPTS is very low as mentioned in introduction section, the burst period should be very long. To compensate for this, the output capacitor of the WPTS must have sufficient capacitance. Nevertheless, when the additional power such as IoT mode is suddenly required in standby mode, the output voltage of WPTS may drop rapidly. To prevent this output voltage drop, burst period should be decided by output voltage monitoring rather than a fixed period and time. As shown in Fig 11, when the output voltage touches the designed voltage, LED can be turned off and the inverter can wake up.

If burst on time is short as shown in Fig 11, the output voltage of WPTS in standby mode may be slightly lower than the output voltage in normal mode due to soft start operation. On the other hand, long burst on-time with high swithcing frequency can increase standby power consumption.

In the proposed system, since the voltage gain is not changed, the input voltage of inverter should be maintained with constant value for WPTS output voltage regulation. If the PFC is turned off in the standby mode, the input voltage of the inverter also changes according to the AC input voltage. In order to compensate for this, burst operation of PFC is also required. The PFC burst period may be synchronized with the inverter burst period, or may operate independently.

4. Experimental Results

4.1 System implementation

Fig. 12 shows a block diagram of the proposed WPTS for TV. The proposed system is divided into three parts (PFC, inverter and Rx board). The PFC

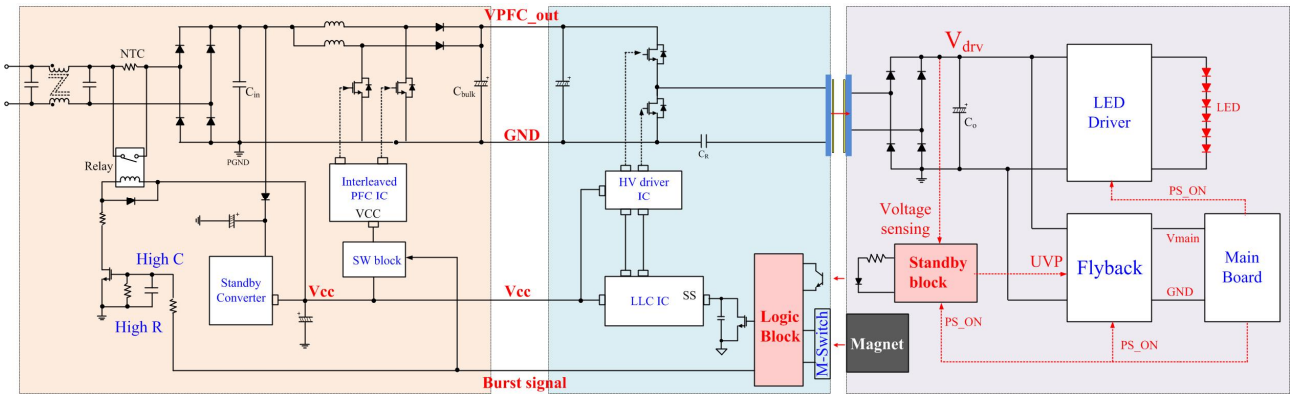

Fig. 12. Block diagram of the proposed WPTS.

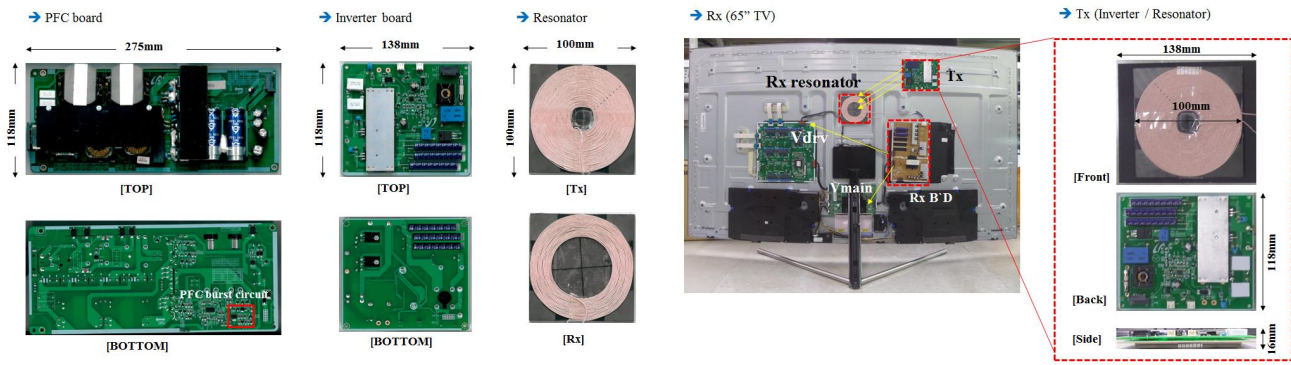

Fig. 13. Photo of prototype sample.

TABLE I
COMPONENTS FOR EXPERIMENT

Block	Item	Part name	Spec. / Description
PFC	Inductor	DS4426	160 uH / DC-bias: 17 A LITZ 0.10 Φ × 180, 27.5 Ts
	FET	MMSF60R190	650 V / 20 A / R_{ds_on}=0.19 Ω
	Diode	U20A6CIC	600 V / 20 A / V_F=1.5 V
	PFC IC	UCC28063	Ineterleaved CrM IC
Inverter	FET	MMSF60R190	650 V / 20 A / R_{ds_on}=0.19 Ω
	LLC IC	UCC25600	LLC control IC
	Driver IC	L6498DTR	HV half-bridge gate IC

TABLE II
SPECIFICATIONS OF RESONATORS

	Do	Di	Wire	Turns	Inductance
Tx	100 mm	25 mm	USTC 0.1Φ x 30	48 Ts	242.1 uH
Rx	100 mm	55 mm	USTC 0.1Φ x 40	22 Ts	91.9 uH

board is implemented with standby converter and circuit for burst operation. In this case, the RC time constant of relay circuit is designed to be very large to suppress the relay noise due to the burst period.

In case of the inverter board, first it is judged whether the Rx device is mounted through the magnet and the magnetic switch, and then the inverter operates with the fixed frequency range.

When an adequate voltage is applied to the receiver, DC-DC converter of receiver operates and supplies power to the main board. After main board power is supplied, an LED driver is operated to control the LED current for TV backlight. Rx also has a standby block, which is used to turn Tx on and off depending on the TV mode status.

Fig. 13 shows a test sample implemented for 65 inch TV and its key components are shown in Table I. The resonator was designed with 100 mm in length. The detailed specifications of the resonator are shown in Table 2. The core is a ferrite core having PL-13 material and its thickness is 2 mm. Table 3 shows the parameter variation of resonator according to misalignment between Tx and Rx resonators.

4.2 Experimental results

Fig. 14 shows key waveforms according to load conditions and distance between Tx and Rx. When

TABLE III
PARAMETER OF RESONATOR ACCORDING TO MISALIGNMENT

	Z-axis misalignment @dx=dy=0mm		X-axis misalignment @dy=0mm, dz=5mm		X-Y axis misalignment @dz=5mm	
	dz=5mm	dz=10mm	dx=5mm	dx=10mm	dx=5mm, dy=5mm	dx=10mm, dy=10mm
L1	466uH	354uH	466uH	504uH	548uH	496uH
L2	160uH	148uH	161uH	150uH	200uH	166uH
L_{lkg}	121uH	169uH	131uH	172uH	190uH	209uH
Coupling coefficient	0.860	0.723	0.848	0.812	0.808	0.761
L_m	401uH	255.9uH	395.1uH	409.1uH	442.9uH	377.3uH
F_R	102kHz	86.6kHz	98.3kHz	85.8kHz	81.6kHz	77.8kHz
Effective turn ratio	1.71	1.55	1.70	1.83	1.66	1.73

the resonators are well-aligned, the inverter is operated at nearly resonance frequency and the magnetizing current is small due to high coupling. When distance is increased, resonant current and magnetizing current are increased due to low coupling.

Fig. 15 shows the measured efficiency and output voltage. As described above, the output voltage is nearly constant at a distance of 5 mm even if the load increases. As the distance becomes longer, the output voltage is somewhat decreased because leakage inductance becomes larger and the resonance frequency becomes lower. However, as shown in Fig. 15, even if the output voltage is reduced, it is possible to operate at a sufficiently high efficiency. However, if some misalignment occurs and high power is required, the efficiency drops sharply as shown in Fig. 15. Therefore, the above-mentioned UVP circuit is required to prevent this. In addition, the X-Y misalignment is more sensitive than Z-misalignment as shown in Fig. 15. Therefore, wider resonator is needed to decrease the sensitivity of X-Y misalignment if high power is required.

Fig. 16 shows the key waveforms in standby mode. As shown in Fig. 16, the PFC and inverter have a very long burst period in the standby mode, and the WPT output voltage swings with lower voltage than the normal mode. Even though it swings at a low voltage level, the well-regulated voltage is supplied to the main board as shown in Fig. 16. Table 4 shows the measured standby power consumption. If Rx is not installed, standby power consumption is very low because only the standby converter operates. If an Rx is installed, inverter operates and standby power consumption increases. However, standby power

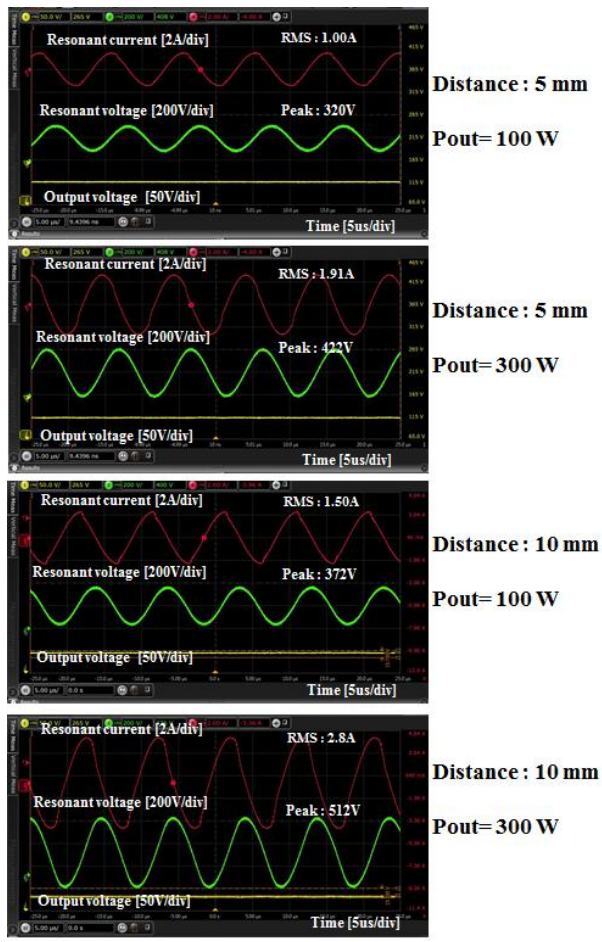

Fig. 14. Key waveforms.

standard for the electronic product (0.5 W ↓) can be sufficiently satisfied.

Fig. 17 shows the waveform when the load of main board increases in standby mode. Since the WPT output voltage is monitored, the burst period is automatically shortened as the load increases, and the output voltage can be well regulated as shown in Fig. 17.

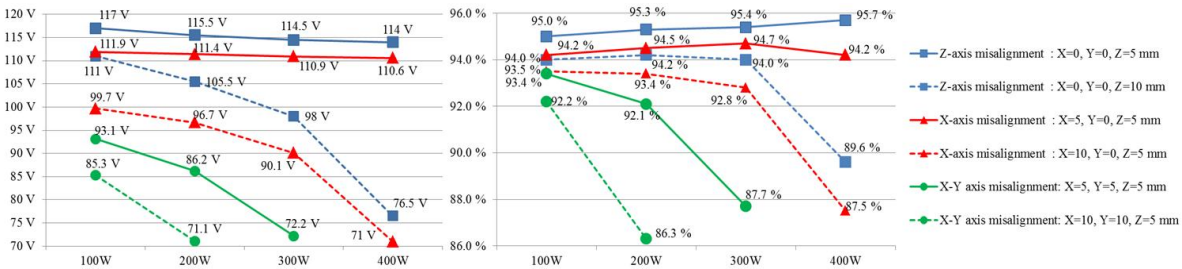

Fig. 15. Measured output voltage and efficiency.

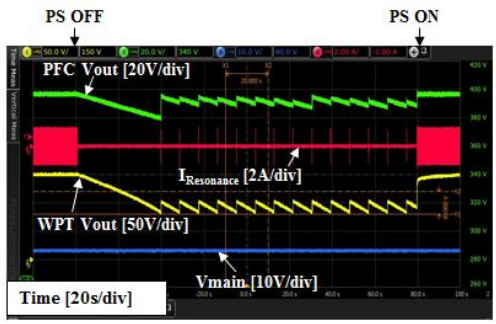

Fig. 16. Key waveforms in standby mode.

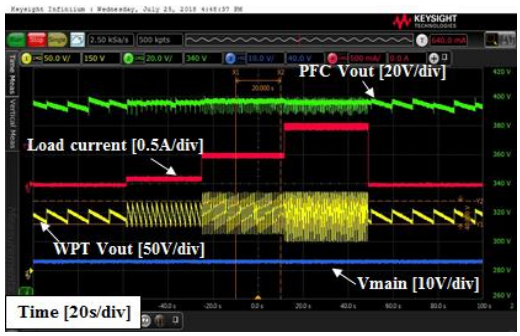

Fig. 17. Load regulation in standby mode.

TABLE Ⅳ
STANDBY POWER CONSUMPTION (@Pout = 125 mW)

	Vin = 115 Vac	Vin = 230 Vac
Rx non-installation	51.2 mW	77.3 mW
Rx Installation	338.5 mW	380.4 mW

5. Conclusion

In this paper, an inductive wireless power transmission system without wireless communication between Tx and Rx is proposed. To eliminate wireless communication module, the Tx and Rx resonators are designed based on the transformer of LLC converter, and the inverter operates in a designed frequency range near the resonance frequency regardless of external factors such as load variations or a misalignment. In the proposed system, the required power can be stably supplied to the authorized devices without wireless communication even though some misalignment occurs.

References

[1] C. S. Wang, O. H. Stielau, and G. A. Covic, "Design considerations for a contactless electric vehicle battery charger," *IEEE Trans. Ind. Electron.*, Vol. 52, No. 5, pp. 1308-1314, Oct. 2005.

[2] J. W. Kim, H. C. Son, D. H. Kim, and Y. J. Park, "Optimal design of a wireless power transfer system with multiple self-resonators for an LED TV," *IEEE Trans. Consum. Electron.*, Vol. 58, No. 3, pp. 775-780, Aug. 2012.

[3] L. Chen, S. Liu, Y. C. Zhou, and T. J. Cui, "An optimizable circuit structure for high-efficiency wireless power transfer," *IEEE Trans. Ind. Electron.*, Vol. 60, No. 1, pp. 339-349, Jan. 2013.

[4] A. P. Sample, D. A. Meyer, and J. R. Smith, "Analysis, experimental results, and range adaptation of magnetically coupled resonators for wireless power transfer," *IEEE Transactions on Industrial Electronics*, Vol. 58, pp. 544-554, 2011.

[5] F. van der Pijl, P. Bauer, and M. Castilla, "Control method for wireless inductive energy transfer systems with relatively large air gap," *IEEE Transactions on Industrial Electronics*, Vol. 60, No. 1, pp. 382-390, Jan. 2013.

[6] W. S. Lee, K. S. Oh, and J. W. Yu, "Distance-insensitive wireless power transfer and near-field communication using a current-controlled loop with a loaded capacitance," *IEEE Transactions on Antennas and Propagation*, Vol. 62, No. 2, pp. 936-940, Feb. 2014.

[7] J. Deng, W. Li, T. D. Nguyen, S. Li, and C. C. Mi, "Compact and efficient bipolar coupler for wireless power chargers: Design and analysis," *IEEE Trans. Power Electron.*, Vol. 30, No. 11, pp. 6130-6140, Nov. 2015.

[8] W. Zhang, S. C. Wong, C. K. Tse, and Q. Chen, "Design for efficiency optimization and voltage controllability of series-series compensated inductive power transfer systems," *IEEE Trans. Power Electron.*, Vol. 29, No. 1, pp. 191-200, Jan. 2014.

[9] K. Colak, E. Asa, M. Bojarski, D. Czarkowski, and O. C.

Onar, “A novel phase-shift control of semibridgeless active rectifier for wireless power transfer,” *IEEE Trans. Power Electron.*, Vol. 30, No. 11, pp. 6288-6297, Nov. 2015.
[10] W. X. Zhong and S. Y. R. Hui, “Maximum energy efficiency tracking for wireless power transfer systems,” *IEEE Trans. Power Electron.*, Vol. 30, No. 7, pp. 4025-4034, Jul. 2015.
[11] T. Diekhans and R. W. D. Doncker, “A dual-side controlled inductive power transfer system optimized for large coupling factor variations and partial load,” *IEEE Trans. Power Electron.*, Vol. 30, No. 11, pp. 6320-6328, Nov. 2015.
[12] J. Huh, W. Y. Lee, S. Y. Choi, G. H. Cho, and C. T. Rim, “Frequency domain circuit model and analysis of coupled magnetic resonance systems,” *Journal of Power Electronics*, Vol. 13, No. 2, pp. 275-286, Mar. 2013.
[13] J. F. Lazar and R. Martinelli, “Steady-state analysis of LLC series resonant converter,” in *Proc. Appl. Power Electron. Conf. Expo. Anaheim, CA*, pp. 728-735. 2001.
[14] B. Yang, F. C. Lee, A. J. Zhang, and G. Huang, “LLC resonant converter for front end DC/DC conversion,” in *Proc. 7th Annu. IEEE Appl. Power Electron. Conf. Expo. Dallas*, TX, pp. 1108-1112, 2002.

Moon-Young Kim

He was born in Korea, in August 1982. He received the B.S. degree from Kyung-Pook National University, Deagu, Korea, in 2008 and the M.S. and Ph.D degrees in electrical engineering from the Korea Advanced Institute of Science and Technology, Daejeon, Korea, in 2010 and 2014, respectively. He is currently a Senior Engineer with Samsung Electronics, Suwon, Korea.

Shin-Wook Choi

He was born in Kwangju, Korea, in July 1982. He received the B.S. degree from Dongguk University, Seoul, in 2008. Since 2010, he has been with Samsung Electronics, the R&D Team of Visual Display Business.

Jeong-il Kang

He was born in Korea, in September 1973. He received his B.S., M.S., and Ph.D. degrees in Electrical Engineering from the Korea Advanced Institute of Science and Technology (KAIST), Daejeon, Korea, in 1995, 1997, and 2002, respectively. In 2002, he joined the Visual Display Business for Samsung Electronics Co., Ltd., Suwon, Korea. Since 2018, he has been working as a Master (Research VP) of Samsung in the area of power electronics, and is currently in charge of the Power Lab as the Head of Lab.

Jonghee Han

He was born in Korea, in March 1962. He received his B.S. degrees in electrical engineering from Inha University, Incheon, Korea. Since joining Samsung in 1988, He has played a significant role in the success of Samsung’s Visual Display business, helping it solidify its top position within the consumer electronics industry. One of his many successes includes continuing the legacy of first place in global market share for 13 consecutive years through continuous development and commercialization of innovative products in TV industry. Mr. Han has accomplished a number of “firsts” in the display industry, serving at the forefront of some of the most noteworthy advancements. For example, he led the development of the world’s first 3D LED TV in 2010 and first Smart TV in 2011, among numerous other developments. More recently, in 2015 he developed the world’s first Quantum Dot TV using environmentally friendly cadmium-free Quantum dot technology and in 2018 further accomplished in creating the world’s first artificial intelligence based QLED 8K TV which delivers superior picture and sound. He also developed core technology of modular based micro LED TV using the world’s first self-luminous element in 2018. In particular, his research specialties include image processing, audio signal processing, analog/digital mixed system, display devices, and power electronics for both innovative display and audio products. He is currently the president of the Visual Display Business for Samsung Electronics.